



Janjua, M. B., Abbas, H. T., Qaraqe, K. A. and Arslan, H. (2023) Beam selection for ambient backscatter communication in beamspace mmWave symbiotic radio. IEEE Wireless Communications Letters, (doi: 10.1109/LWC.2023.3235104).

There may be differences between this version and the published version. You are advised to consult the publisher's version if you wish to cite from it.

<https://eprints.gla.ac.uk/289038/>

Deposited on: 5 January 2023

Enlighten – Research publications by members of the University of Glasgow
<https://eprints.gla.ac.uk>

Beam Selection for Ambient Backscatter Communication in Beamspace mmWave Symbiotic Radio

Muhammad Bilal Janjua, *Student Member, IEEE*, Hasan T. Abbas, *Senior Member, IEEE*, Khalid Qaraqe, *Senior Member, IEEE*, Hüseyin Arslan, *Fellow, IEEE*

Abstract—The Internet of Things revolution has profoundly impacted wireless communication systems. Access to a high data rate is now just as important as low power operation. The use of incident millimeter-wave (mmWave) signals for ambient backscatter communication (AmBC) has shown significant promise for delivering high data rates. However, incident signal availability to a backscatter devices (BDs) at mmWave is erratic due to channel sparsity. In order to address the incident signal inaccessibility problem and enable high data-rate AmBC, this paper presents an efficient beam selection method in the beamspace millimeter-wave symbiotic radio system. The proposed method improves the overall system’s sum-rate performance by up to 30% with signals accessibility to BDs.

Index Terms—Ambient backscatter communication, mmWave symbiotic radio, beam selection, beamspace MIMO.

I. INTRODUCTION

We are witnessing great technological strides in a wide-ranging adaptation of the Internet of things (IoT). As a result, more and more devices are going online, and the demand for the electromagnetic spectrum is now more than ever. In recent years, we have witnessed the inclusion of IoT in various systems such as healthcare, education, industry, agriculture, transportation, and so on [1]. Until now, IoT devices are considered to have low data rate and energy efficiency requirements. However, with the development of extended reality, a high data rate has become another critical requirement, particularly in the case of wearable devices, e.g., XR glasses [2].

Ambient backscatter communication (AmBC) is considered a revolutionary energy-efficient technology for sixth-generation (6G) and beyond wireless systems [3]. Although AmBC system can substantially enhance the energy efficiency, its dependency on the signals of existing wireless systems poses a great question on its reliability. Recently, a symbiotic radio (SRad) is proposed to avoid interference and enable cooperative resource sharing between AmBC system and existing

wireless systems [4]. In SRad, both systems can share the resources through different relationships to benefit each other.

On the other hand, millimeter-wave (mmWave) frequency bands offer large bandwidths and provide very high data rates and long-range communication with the support of massive multiple-input multiple-output (MIMO) systems. Although these technologies are the key enablers of fifth-generation (5G) and beyond wireless systems, their full potential has not been experienced yet due to significant energy consumption, and hardware cost comes from radio-frequency radio-frequency (RF) chains required to support a massive number of antennas. To overcome this problem, a beamspace MIMO system has been proposed to exploit the channel sparsity at mmWave frequency. In the beamspace MIMO, significantly contributing beams are selected from the sparse channel to reduce the number of RF chains and enhance the energy efficiency gains [5], [6]. The conventional beam selection schemes are not suitable in case of mmWave AmBC system, since backscatter devices (BDs) may exist in less contributing beams and be out of coverage.

SRad combines the benefits of mmWave and AmBC to achieve low-power high data rate communication. In [7], a mmWave SRad with single BD is proposed to achieve high data rate in AmBC. In particular, a joint hybrid and passive beamforming is performed at mmWave transmitter (Tx) and BD. Unlike this work, our aim is to provide the RF signal accessibility to BDs while selecting the beams for a user in mmWave SRad system.

There are two main contributions of the paper to the mmWave SRad state-of-the-art,

- This is the first study that proposes a beam selection based solution to address the problem of ambient RF signal inaccessibility at BDs in beamspace mmWave SRad system.
- This work leverages a magnitude maximization-based beam selection approach considering the channel gains of both BD and ordinary scatterers to enhance sum-rate performance of the system.

II. MMWAVE SRAD MODELLING

A. System Model

We consider a SRad with an AmBC system in symbiosis with a mmWave MIMO communication system. Both system shares the radio resource at signal level and have a common

M. B. Janjua is with the Department of Electrical and Electronics Engineering, Istanbul Medipol University, Istanbul, 34810, Turkey and also with the Department of Electrical and Computer Engineering, Texas A&M University at Qatar, Doha, Qatar (email: muhammad.janjua@std.medipol.edu.tr). H. T. Abbas is with James Watt School of Engineering, University of Glasgow, Glasgow G12 8QQ, U.K. (email: hasan.abbas@glasgow.ac.uk). K. Qaraqe is with the Department of Electrical and Computer Engineering, Texas A&M University at Qatar, Doha, Qatar. (email: khalid.qaraqe@qatar.tamu.edu). H. Arslan is with the Department of Electrical and Electronics Engineering, Istanbul Medipol University, Istanbul, 34810, Turkey (email: huseyin-arслан@medipol.edu.tr).

receiver (Rx). AmBC system consists of single antenna passive BDs i.e., IoT devices, which utilize the incident RF signal generated by mmWave Tx and sends its data to the cooperative mmWave Rx. There are N_{Tx} and N_{Rx} antenna elements at Tx and Rx in mmWave system, respectively. Each antenna element has uniform radiation in all directions.

B. Channel Model

We assume a sparse narrowband mmWave MIMO communication channel with only a few scattering clusters¹ due to propagation characteristics of signals in mmWave frequencies [8]. In contrast to the traditional mmWave MIMO system, scatterers can either be common scattering objects or BDs in SRad. As a result, we divide the scattering clusters into three categories, as depicted in Fig. 1. Similar to normal clusters represented in mmWave MIMO systems, the first type of cluster has just ordinary scatterers as outside sources. Ordinary scatterers and BDs both exist in the second cluster type, but BDs are the only objects in the third cluster type. However, there is only one path from either a BD or a ordinary scatterer in each cluster at mmWave bands due to the high channel sparsity. Thus, channel between Tx and Rx is modelled according to the extended Saleh-Valenzuela model [9],

$$\mathbf{H} = \sqrt{\frac{N_{Rx}N_{Tx}}{N_p}} \sum_{p=1}^{N_p} \alpha_p \mathbf{a}_{Rx}(\phi_{R,p}) \mathbf{a}_{Tx}^H(\phi_{T,p}), \quad (1)$$

where $\mathbf{H} \in \mathbb{C}^{N_{Rx} \times N_{Tx}}$ represents the channel between Rx and Tx, α_p with $p = 1, 2, \dots, N_p$, $\mathbf{a}_{N_{Rx}}(\phi_{R,p}) \in \mathbb{C}^{N_{Rx} \times 1}$, and $\mathbf{a}_{N_{Tx}}(\phi_{T,p}) \in \mathbb{C}^{N_{Tx} \times 1}$ are the complex path gain, steering vectors for angle-of-arrival (AoA) $\phi_{R,p}$ and angle-of-departure (AoD) $\phi_{T,p}$ of the p -th path, respectively. Furthermore, uniform linear array (ULA) of antennas are considered at Tx and Rx in a horizontal placement, and $\phi_{R,p}$ and $\phi_{T,p}$ are azimuth AoA and AoD of the p -th path. The array steering vector $\mathbf{a}_t(\phi)$ at $t \in \{\text{Tx}, \text{Rx}\}$ for $N_t \in [N_{Tx}, N_{Rx}]$ antenna elements in ULA and can be described as [5],

$$\mathbf{a}_{N_t}(\phi) = \frac{1}{\sqrt{N_t}} [e^{-j2\pi\phi i}]_{i \in \mathcal{I}(N_t)} \quad (2)$$

where $\mathcal{I}(N_t) = \{i - (N_t - 1)/2, i = 0, 1, \dots, N_t - 1\}$ gives the symmetric set of indices for a pre-specified value of N_t , $\phi = \frac{\Omega \sin(\theta)}{\lambda}$ represents the spatial beamforming directions between ranges $-\frac{1}{2} \leq \phi \leq \frac{1}{2}$ and θ describes the physical direction of the beams covering the entire spatial area $-\frac{\pi}{2} \leq \theta \leq \frac{\pi}{2}$. Ω denotes the antenna element spacing with $\Omega = \lambda/2$, while λ is the wavelength.

As there can be ordinary scatterers or BDs in the paths (i.e., $p \in [b, l]$), we define $N_p = N_b + N_l$, where N_b , and N_l denote number of BDs and number of ordinary scatterers, respectively, which contribute to the N_p paths. In case there are no BDs, then $N_b = 0$ and $N_p = N_l$. Similarly, when there are only BDs, then $N_p = N_b$ and $N_l = 0$. In all three cases, contributing scatterers are assumed to be non-vanishing, and exist in the far-field of Tx and Rx. Besides, the number of

¹We consider the clusters generated from single-bounce reflections only.

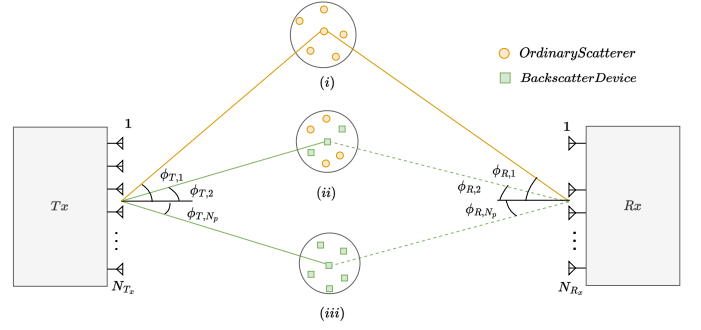


Fig. 1. The mmWave MIMO SRad system model with three different types of scatterers in the cluster: i) ordinary scatterers; ii) BDs in ordinary scatterers; iii) only BDs.

paths are less than transmit and receive antennas (i.e., $N_p \leq N_{Rx} \leq N_{Tx}$). In our proposed system, each path between Tx and Rx represents a channel of a BD or an ordinary scatterer, (1) is rewritten as,

$$\mathbf{H} = \gamma \left(\sum_{b=1}^{N_b} \alpha_b \mathbf{a}_{Rx}(\phi_{R,b}) \mathbf{a}_{Tx}^H(\phi_{T,b}) + \sum_{l=1}^{N_l} \alpha_l \mathbf{a}_{N_{Rx}}(\phi_{R,l}) \mathbf{a}_{N_{Tx}}^H(\phi_{T,l}) \right), \quad (3)$$

where $\gamma = \sqrt{\frac{N_{Rx}N_{Tx}}{N_b + N_l}}$ is the normalization factor. To describe the channel in a matrix form, (3) can also be written as,

$$\mathbf{H} = \mathbf{A}_{Rx} \Delta_b \mathbf{A}_{Tx}^H + \mathbf{A}_{Rx} \Delta_l \mathbf{A}_{Tx}^H \quad (4)$$

where $\mathbf{A}_{Rx} = [\mathbf{a}_{Rx}(\phi_{R,1}), \dots, \mathbf{a}_{Rx}(\phi_{R,N_p})]$ and $\mathbf{A}_{Tx} = [\mathbf{a}_{Tx}(\phi_{T,1}), \dots, \mathbf{a}_{Tx}(\phi_{T,N_p})]$ are the array response matrices of Rx and Tx, respectively, $\Delta_b = \gamma \text{diag}[\alpha_{11} \quad \alpha_{bb} \quad \alpha_{N_b N_b} \quad 0_{ll} \quad 0_{N_l N_l}]$, and $\Delta_l = \gamma \text{diag}[0_{11} \quad 0_{bb} \quad 0_{N_b N_b} \quad \alpha_{ll} \quad \alpha_{N_l N_l}]$ are matrices consist of the complex path gains of BDs and ordinary scatterers, respectively.

Now to obtain the finite dimensionality of the mmWave massive MIMO system, a beamspace representation is used with fixed beamforming at Tx and Rx. By multiplying with discrete Fourier transform matrices \mathbf{U}_{N_t} at Tx and Rx, we can transform \mathbf{H} to beamspace [10],

$$\mathbf{U}_{N_t} = [\mathbf{a}_{N_t}(\hat{\phi}_1), \mathbf{a}_{N_t}(\hat{\phi}_2), \dots, \mathbf{a}_{N_t}(\hat{\phi}_{N_t})] \quad (5)$$

\mathbf{U}_{N_t} is a $N_t \times N_t$ unitary matrix with $\mathbf{U}_{N_t}^H \mathbf{U}_{N_t} = \mathbf{U}_{N_t} \mathbf{U}_{N_t}^H = \mathbf{I}$, and $\hat{\phi}_v = \frac{1}{N_t} (v - \frac{N_t+1}{2})$ for $v = 1, 2, \dots, N_t$ are pre-defined spatial directions. Thus, beamspace channel representation is described as,

$$\tilde{\mathbf{H}} = \mathbf{U}_{N_{Rx}}^H \mathbf{H} \mathbf{U}_{N_{Tx}}, \quad (6)$$

where $\tilde{\mathbf{H}}$ denotes the beamspace channel. By converting the channel into beamspace domain, the dimension of the channel matrix reduces to the subspace of the beams. From the beamspace channel, we can select the beams that contribute to BDs' paths to provide them signal accessibility, as well as the beams for ordinary scatterers with strong path gains.

C. BD Modulation and Joint Rx Design

Let \mathbf{x} be the signal transmitted by Tx to Rx in the direction of BDs and ordinary scatterers. BD transmits its information signal $q_b \sim \mathcal{N}(0, 1)$ by modulating the incident beam coming from Tx [11]. The modulation at BD is performed by changing the load impedance and switching the antenna into reflecting and non-reflecting states. Specifically, the backscatter modulation at b -th BD with antenna switching can be expressed by the antenna reflection coefficient Γ_b^s defined as,

$$\Gamma_b^{(c)} = \frac{Z_{L,b}^{(c)} - Z_{a,b}^*}{Z_{L,b}^{(c)} + Z_{a,b}}, \quad (7)$$

where $Z_{L,b}^{(c)}$ is the load impedance, $Z_{a,b}$ is the antenna impedance of b -th BD, $*$ is the complex conjugate, and $c = 1, 2$ are the switch states. We assume the information bit zero '0' is represented by load impedance matching with the antenna impedance i.e., $Z_{L,b}^{(c)} = Z_{a,b}^*$, when antenna absorbs the RF signal. On the other hand, the information bit one '1' is represented by impedance mismatch i.e., $Z_{L,b}^{(c)} \neq Z_{a,b}^*$, when antenna completely reflects the RF signal. $\Gamma_b^{(c)} \in [0, 1]$ controls the backscattered signal power at BD and q_b is scaled up as $\Gamma_b^{(c)} q_b$. The signal sent by the Tx after being re-modulated by BDs and scattered by ordinary scatterers can be expressed in the antenna domain at Rx as,

$$\mathbf{y} = \mathbf{H}\mathbf{x} + \mathbf{z} \quad (8)$$

$$= (\mathbf{A}_{Rx} \Delta_b^q \mathbf{A}_{Tx}^H + \mathbf{A}_{Rx} \Delta_l \mathbf{A}_{Tx}^H) \mathbf{x} + \mathbf{z}$$

where $\mathbf{y} \in \mathbb{C}^{N_{Rx} \times 1}$ is the received signal vector, $\mathbf{x} \in \mathbb{C}^{N_{Tx} \times 1}$ is the signal vector transmitted by Tx, $\Delta_b^q = \text{diag}([\alpha_1 \Gamma_1^{(c)} q_1 \quad \alpha_2 \Gamma_2^{(c)} q_2 \quad \dots \quad \alpha_{N_b} \Gamma_{N_b}^{(c)} q_{N_b} \quad 0_{bb} \quad 0_{N_l N_l}])$ represent the signal vector of all BDs', and $\mathbf{z} \sim \mathcal{CN}(0, \sigma^2 \mathbf{I})$ represents the noise vector. The system model provided in (8) can be re-written in equivalent beamspace representation,

$$\tilde{\mathbf{y}} = \tilde{\mathbf{H}}\tilde{\mathbf{x}} + \tilde{\mathbf{z}}$$

$$= \mathbf{U}_{N_{Rx}}^H (\mathbf{A}_{Rx} \Delta_b^q \mathbf{A}_{Tx}^H + \mathbf{A}_{Rx} \Delta_l \mathbf{A}_{Tx}^H) \mathbf{U}_{N_{Tx}} \tilde{\mathbf{x}} + \tilde{\mathbf{z}} \quad (9)$$

$$= (\tilde{\mathbf{H}}_{Rx,b} \Delta_b^q \tilde{\mathbf{H}}_{Tx,b} + \tilde{\mathbf{H}}_{Rx,l} \Delta_l \tilde{\mathbf{H}}_{Tx,l}) \tilde{\mathbf{x}} + \tilde{\mathbf{z}},$$

where $\tilde{\mathbf{y}} = \mathbf{U}_{N_{Rx}}^H \mathbf{y}$, $\tilde{\mathbf{x}} = \mathbf{U}_{N_{Tx}}^H \mathbf{x}$, and $\tilde{\mathbf{z}} = \mathbf{U}_{N_{Rx}}^H \mathbf{z}$, are the received signal, transmitted signal and noise vectors in the beamspace, respectively. $\tilde{\mathbf{H}}_{Tx,b} (\tilde{\mathbf{H}}_{Tx,l})$ represent beamspace channel matrix between Tx and BD (ordinary scatterers), and $\tilde{\mathbf{H}}_{Rx,b} (\tilde{\mathbf{H}}_{Rx,l})$ denote beamspace channel matrix between Rx and BDs (ordinary scatterers).

III. BEAM SELECTION AT TX AND RX

In this section we present the beam selection at the Tx and Rx based on the magnitude maximization. In particular, the channels with the high gains are selected at Tx and Rx considering the path gains of ordinary scatterers and signal accessibility to BDs. Additionally, we assume that Tx and Rx have access to perfect channel state information for BDs links and ordinary scatterers' paths. A sparsity mask is defined at Tx and Rx that determines the dominating beams traveling along a specific path in order to select the beams. The sparsity mask for b -th backscatter is described as,

$$\mathcal{M}_{b,t} = \left\{ i \in \mathcal{I}(N_t) : |h_{t,b}(i)|^2 \geq \zeta_b \max_i |h_{t,b}(i)|^2 \right\}$$

$$\tilde{\mathcal{M}}_t = \bigcup_{b=1, \dots, N_b} \mathcal{M}_{b,t}, \quad (10)$$

where $\mathcal{M}_{b,t}$ represents the sparsity mask for b -th BD at Tx/Rx, defined based on threshold $\zeta_b \in [0, 1]$, $h_{t,b}$ is the channel gain between b -th BD and $t \in \{Tx, Rx\}$, and $\tilde{s}_t = |\tilde{\mathcal{M}}_t|$ represents set of selected beams at t . Similarly, for the l -th ordinary scatterer, the mask can be defined as,

$$\mathcal{M}_{l,t} = \left\{ i \in \mathcal{I}(N_t) : |h_{t,l}(i)|^2 \geq \zeta_l \max_i |h_{t,l}(i)|^2 \right\}$$

$$\hat{\mathcal{M}}_t = \bigcup_{l=1, \dots, N_l} \mathcal{M}_{l,t}, \quad (11)$$

where $\mathcal{M}_{l,t}$ represents the sparsity mask for l -th ordinary scatterer that is defined by a threshold ζ_l , $h_{t,l}$ is the channel gain between t and l -th ordinary scatterer, and $\hat{s}_t = |\hat{\mathcal{M}}_t|$ represents the set of beams selected at t . The set $s_t = |\mathcal{M}_t|$ of all selected beams for both BDs and ordinary scatterers at Tx/Rx is given by,

$$\mathcal{M}_t = \tilde{\mathcal{M}}_t \bigcup \hat{\mathcal{M}}_t. \quad (12)$$

Through the beam selection using the magnitude maximization approach, the received signal with a low-dimensional channel is represented as,

$$\tilde{\mathbf{y}} = \bar{\mathbf{H}}\tilde{\mathbf{x}} + \tilde{\mathbf{z}}; \quad \bar{\mathbf{H}} = \mathbb{H}_b + \mathbb{H}_l, \quad (13)$$

where $\mathbb{H}_b = [\tilde{\mathbf{H}}_{Rx,b}(j, \cdot) \Delta_b^q \tilde{\mathbf{H}}_{Tx,b}(j, \cdot)]_{j \in \tilde{\mathcal{M}}_t}$ and $\mathbb{H}_l = [\tilde{\mathbf{H}}_{Rx,l}(k, \cdot) \Delta_l \tilde{\mathbf{H}}_{Tx,l}(k, \cdot)]_{k \in \hat{\mathcal{M}}_t}$ are $s_{Rx} \times s_{Tx}$ channel matrices corresponding to the selected beams for BDs and ordinary scatterers.

We measure the performance of the proposed beam selection scheme in terms of achievable sum-rate. To simplify the notation, from now on we will use $p \in \{b, l\}$ instead of b and l as defined in (1). Rx considers the signal of BDs as interference and estimates its sum-rate in the following manner,

$$R_{Rx} = \log_2 \det \left(\mathbf{I} + \frac{\rho |\beta|^2}{N_p} \mathbf{G}_{Rx}^H \bar{\mathbf{H}} \bar{\mathbf{H}}^H \mathbf{G}_{Tx} \mathcal{R}^{-1} \right) \quad (14)$$

where $G_t = \beta \mathbf{F}_t = \beta [\mathbf{f}_{t,1}, \mathbf{f}_{t,p}, \dots, \mathbf{f}_{t,N_p}]$ denotes the precoder for $t = Tx$ and filter matrix for $t = Rx$, respectively. In case of linear transceivers we use $\mathbf{F} = \mathbf{H}$ as a matched filter. β satisfies the total power constraint as follows $\beta = \sqrt{\frac{\rho}{\text{tr}(\mathbf{F}_{Tx}^H \Delta_p \mathbf{F}_{Tx})}}$, \mathcal{R}^{-1} represents the signal-to-interference-plus-noise (SINR) ratio signal, which is,

$$\mathcal{R}^{-1} = \sigma_n^2 + \frac{\rho |\beta|^2}{N_p} \mathbf{G}_{Rx}^H \mathbb{H}_b \mathbb{H}_b^H \mathbf{G}_{Tx} \quad (15)$$

After performing the perfect successive interference cancellation of Rx signal \mathbf{x} , the sum-rate of the b -th BD can be measured as,

$$R_b = \log_2 (1 + \text{SINR}_b) \quad (16)$$

$$\text{SINR}_b = \frac{\frac{\rho |\beta|^2}{N_p} |\mathbf{f}_{Rx,p}^H \mathbf{h}_{Rx,p} \Delta_p \mathbf{h}_{Tx,p}^H \mathbf{f}_{Tx,p}|^2}{\frac{\rho |\beta|^2}{N_p} \sum_{m \neq \{p\}} |\mathbf{f}_{Rx,m}^H \mathbf{h}_{Rx,p} \Delta_m \mathbf{h}_{Tx,p}^H \mathbf{f}_{Tx,m}|^2 + \sigma_n^2}} \quad (17)$$

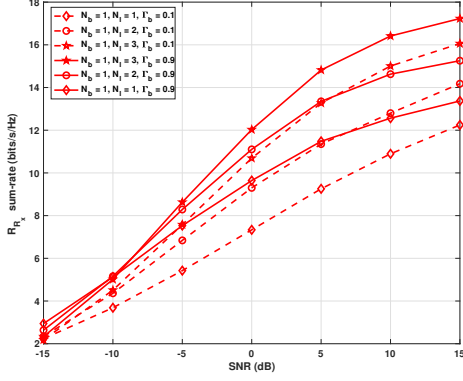


Fig. 2. R_{R_x} sum-rate vs SNR for single BD and multiple ordinary scatterers.

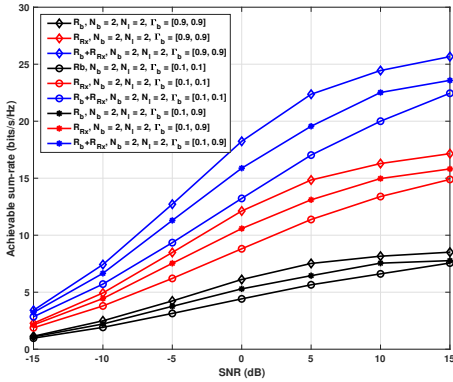


Fig. 3. Achievable sum-rate vs SNR for multiple BDs and multiple ordinary scatterers.

IV. SIMULATION RESULTS AND DISCUSSIONS

We consider the following set of parameters for the simulations: $N_{Tx} = 256$, $N_{Rx} = 16$, $N_p = 4$. The path gains $|\alpha_b|^2$ and $|\alpha_l|^2$ are considered to be between -5 dB to -10 dB for single bounce paths [10]. Furthermore, we assume $\Gamma_b = 0.1$ when the BD is in non-reflecting state and $\Gamma_b = 0.9$ when BD is in reflecting state.

Figure 2 shows the sum-rate of Rx i.e., R_{R_x} with $N_b = 1$ and $N_l = 1, 2, 3$. The number of selected beams at Tx and Rx are according to N_b and N_l in each case. It is seen in that value of R_{R_x} is maximum when $N_l = 3$ and $\Gamma_b = 0.9$. For instance, at 10 dB of SNR, R_{R_x} is around 16 bits/sec/Hz when $N_b = 1, N_l = 3, \Gamma_b = 0.9$ but it drops to 15 bits/sec/Hz when $\Gamma_b = 0.1$. Besides, R_{R_x} also decreases with the decreasing value of N_l ; for example it reduces to 11 bits/sec/Hz with $N_l = 1$ and $\Gamma_b = 0.1$. Figure 3 shows the achievable sum-rate of SRad system with multiple BDs and ordinary scatterers. The sum-rate is obtained with different values of N_b , and N_l . For example, at a signal-to-noise-ratio (SNR) value of 10 dB the highest values of R_b , R_x and $R_b + R_x$ are achieved when $N_b = N_l = 2$, and all BDs transmit with the maximum reflection coefficient $\Gamma_b = [0.9, 0.9]$. As one BD reflects with low reflection coefficient i.e., $\Gamma_b = [0.1, 0.9]$, which means it is not contributing, so the sum-rate decreases to minimum

when both BDs are not contributing with $\Gamma_b = [0.1, 0.1]$. Furthermore, Fig. 3 shows that BDs with $\Gamma_b = [0.9, 0.9]$ improve the achievable sum-rate of the system up to 30% compared to BDs with $\Gamma_b = [0.1, 0.1]$. Thus, simulation results validate the sum-rate enhancement with the beam-selection and also the selection of the paths with different type of scatterers such as BD and ordinary scatterers in the environment.

V. CONCLUSION

In this letter, we proposed a beam selection scheme to maximize the RF signal accessibility to backscatter devices in the mmWave SRad system. As the AmBC system relies on the signals of ambient RF sources, resource availability is crucial for such a system to operate. Due to the sparsity of the mmWave channel, the incident signal may be inaccessible to BDs to support their communication. Therefore, a beam selection in the beamspace domain is performed based on the magnitude maximization of the channel and choosing the strongest paths between Tx and Rx while ensuring the signal accessibility to BDs. The performance of the beam selection scheme is measured in terms of the achievable sum-rate of the system. The simulation results validated that when beams are selected considering BDs result in sum-rate enhancement of the overall system. Future studies may consider the interference issues when the same beam is selected for multiple BDs.

REFERENCES

- [1] L. Zhang, Y.-C. Liang, and M. Xiao, "Spectrum sharing for Internet of Things: A survey," *IEEE Wireless Commun.*, vol. 26, no. 3, pp. 132–139, 2018.
- [2] M. Maier, A. Ebrahimzadeh, S. Rostami, and A. Beniche, "The Internet of No Things: Making the Internet Disappear and" See the Invisible"," *IEEE Commun. Mag.*, vol. 58, no. 11, pp. 76–82, 2020.
- [3] I. F. Akyildiz, A. Kak, and S. Nie, "6G and beyond: The future of wireless communications systems," *IEEE Access*, vol. 8, pp. 133 995–134 030, 2020.
- [4] M. B. Janjua and H. Arslan, "Survey on Symbiotic Radio: A Paradigm Shift in Spectrum Sharing and Coexistence," *arXiv preprint arXiv:2111.08948*, 2021.
- [5] A. Sayeed and J. Brady, "Beamspace MIMO for high-dimensional multiuser communication at millimeter-wave frequencies," in *Proc. IEEE Global Commun. Conf. (GLOBECOM)*, Dec. 2013, pp. 3679–3684.
- [6] P. V. Amadori and C. Masouros, "Low RF-complexity millimeter-wave beamspace-MIMO systems by beam selection," *IEEE Trans. Commun.*, vol. 63, no. 6, pp. 2212–2223, 2015.
- [7] G. Yang, T. Wei, and Y.-C. Liang, "Joint Hybrid and Passive Beamforming for Millimeter Wave Symbiotic Radio Systems," *IEEE Wireless Commun. Lett.*, vol. 10, no. 10, pp. 2294–2298, 2021.
- [8] T. S. Rappaport, S. Sun, R. Mayzus, H. Zhao, Y. Azar, K. Wang, G. N. Wong, J. K. Schulz, M. Samimi, and F. Gutierrez, "Millimeter wave mobile communications for 5G cellular: It will work!" *IEEE Access*, vol. 1, pp. 335–349, 2013.
- [9] O. El Ayach, S. Rajagopal, S. Abu-Surra, Z. Pi, and R. W. Heath, "Spatially sparse precoding in millimeter wave MIMO systems," *IEEE Trans. Wireless Commun.*, vol. 13, no. 3, pp. 1499–1513, 2014.
- [10] G. H. Song, J. Brady, and A. Sayeed, "Beamspace MIMO transceivers for low-complexity and near-optimal communication at mm-wave frequencies," in *Proc. IEEE Int. Conf. Acoust. Speech Signal Process.*, May 2013, pp. 4394–4398.
- [11] B. Clerckx, Z. B. Zawawi, and K. Huang, "Wirelessly powered backscatter communications: Waveform design and SNR-energy tradeoff," *IEEE Commun. Lett.*, vol. 21, no. 10, pp. 2234–2237, 2017.